Proceedings of the
2007 IEEE Intelligent Vehicles Symposium
Istanbul, Turkey, June 13-15, 2007

Slip Control for Vehicles Platooning via Second Order Sliding Modes

Matteo Amodeo, Antonella Ferrara, Riccardo Terzaghi and Claudio Vecchio

Abstract— **Recent research has demonstrated that longitudinal control strategies are useful in highway systems to regulate the spacing and velocity of vehicles. In this paper, a robust longitudinal control system for platoons of vehicles is designed. The proposed control scheme is composed of two different loops: the outer loop has to determine the traction force necessary to maintain the safety distance between the controlled vehicle and the preceding vehicle, while the inner loop is aimed at producing the desired traction force, calculated by the outer loop, by controlling the slip ratio. The unknown time–varying road conditions are taken into account by using an adaptive algorithm. The proposed controller enforces second order sliding modes, and, in contrast to conventional sliding mode controllers generates continuous control actions, thus resulting particularly suitable to be applied to automotive systems, where vibrations limitation is a crucial requirement.**

I. Introduction

Recent research has shown that longitudinal control of platoons of vehicles is effective to improve the traffic capacity of road networks, while maintaining safety distances between vehicles [15]. The platoon control problem has been extensively discussed and numerous longitudinal control systems have been proposed in the literature (see, for instance [3], [5], [6], [11] and the references therein). However, not all the work on platoon control sufficiently emphasize the influence of the tire/road interaction on the vehicle longitudinal motion.

In practical applications, the tire/road interaction needs to be explicitly taken into account in order to increase vehicle stability, allowing anti–skid braking and anti–spin acceleration, so that vehicle performances can be greatly improved. Since the tire/road surface interaction is unknown and time–varying, an adaptive control algorithm can be adopted to on–line determine the tire/road adhesion coefficient. A valid proposal, based on a recursive least–squares approach, is described in [13].

On the other hand, due to system uncertainties and the wide range of operating conditions, which are typical of the automotive context, a robust control technique is required to address the considered problem. Many proposals are based on sliding mode control (see, for instance, [5], [9], [12], [13], [18]). Yet, conventional sliding mode control laws produce discontinuous control inputs. By directly acting on the throttle and the brakes through a discontinuous control law, high frequency chattering is produced, which can generate excessive mechanical wear and passengers' discomfort, due to the propagation of vibrations throughout the different subsystems of the controlled vehicle. A possible counteraction to eliminate or, at least, reduce the vibrations induced by the controller consists in the approximation of the discontinuous control signals with continuous ones. This is for instance the solution adopted in [13]. However, because of the approximation, the sliding modes cannot be actually enforced, so that the controlled system state evolve in a boundary layer of the ideal sliding subspace, featuring a dynamical behaviour possibly quite different from that attainable if ideal sliding modes could be generated.

The idea investigated in this work is to exploit the positive features of second order sliding mode (SOSM) control [2] to solve the platooning problem. The proposed SOSM controller generates a continuous control action, but the enforced sliding mode is ideal, in contrast to what happens for solutions which relies on continuous approximations of the discontinuous control laws. This allows us to circumvent the inconvenient of the vibrations induced by conventional sliding mode controllers. Moreover, one of the objective of the present work is to keep into account the time–varying tire/road interaction while performing the control task.

The proposed control scheme is designed for each vehicle of the platoon, apart from the leader vehicle which is autonomous. It is composed of two control loops as depicted in Fig. 1. The control objective of the outer loop is to generate a desired traction force in order to maintain the correct spacing between the controlled vehicle and the preceding vehicle. The tire traction force depends on the wheel slip λ, and on the road surface conditions. It is assumed that reliable measurements of the vehicle speed and of the wheel angular velocity, which allow for an accurate determination of the wheel slip, are available [16], [9]. Thus, the desired traction force in the longitudinal direction can be generated by controlling the wheel slip. The desired slip ratio is calculated on the basis of the desired traction force generated by the outer control loop, and on the current tire–road adhesion coefficient. This value is determined on–line using a recursive least–square technique, according to the approach described in [13]. The inner loop is composed of a slip controller that tracks the desired slip ratio by acting on the torques at the front and rear wheels.

The paper is organised as follows. Section II is devoted to introduce the model of the vehicle, to specify the assumptions, and to state the control objectives. Section III briefly revises the basic concepts of second order sliding mode control. The design of the second order sliding mode controller is discussed in Sections IV and V. Some comments about the proposed control scheme are given in Section VI. Simulation results relevant to a platoon composed of two

A. Ferrara and C. Vecchio are with the Department of Computer Engineering and Systems Science, University of Pavia, Via Ferrata 1, 27100 Pavia, Italy. e-mail:{antonella.ferrara, claudio.vecchio}@unipv.it.

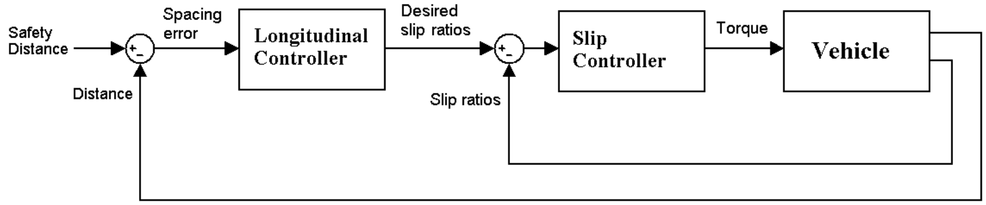

Fig. 1. The proposed control scheme of each vehicle.

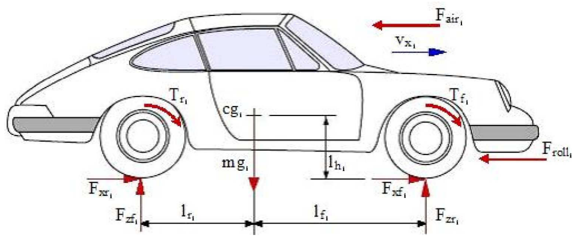

Fig. 2. The vehicle model.

vehicles is reported in Section VII. Some conclusions are gathered in the last section.

II. The vehicle model

The platoon considered in this paper is composed of $n+1$ vehicles. The 0–th vehicle is the so–called leader vehicle which is autonomously driven by its driver. The vehicle model used for the design of the controller is a nonlinear single–track model [8], that is, the longitudinal dynamics of the i–th vehicle within the platoon is given by the following equations

$$\begin{aligned}
m_i\dot{v}_{x_i} &= 2[F_{xf_i}(\lambda_{f_i})+F_{xr_i}(\lambda_{r_i})]-F_{loss_i}(v_{x_i}) && (1)\\
J_{f_i}\dot{\omega}_{f_i} &= T_{f_i}-r_{f_i}F_{xf_i}(\lambda_{f_i}) && (2)\\
J_{r_i}\dot{\omega}_{r_i} &= T_{r_i}-r_{r_i}F_{xr_i}(\lambda_{f_i}) && (3)\\
F_{loss_i}(v_{x_i}) &= F_{air_i}(v_{x_i})+F_{roll_i} && (4)\\
&= c_{x_i}v_{x_i}^2\cdot sign(v_{x_i})+f_{roll_i}m_ig\\
F_{zf_i} &= \frac{l_{r_i}m_ig-l_{h_i}m_i\dot{v}_{x_i}}{2(l_{f_i}+l_{r_i})} && (5)\\
F_{zr_i} &= \frac{l_{f_i}m_ig+l_{h_i}m_i\dot{v}_{x_i}}{2(l_{f_i}+l_{r_i})} && (6)
\end{aligned}$$

where v_{x_i} is the longitudinal velocity, ω_i is the wheel angular velocity, T_i is the input torque on a wheel, F_{x_i} is the traction force on a wheel, F_{z_i} is the normal force on a wheel, approximated in this work as a static value, F_{air_i} is the air drag, and F_{roll_i} is the rolling resistance (see Fig. 2). Subscripts f and r denote 'front tire' and 'rear tire', respectively. As for the vehicle parameters: m_i is the vehicle mass, c_{x_i} is the longitudinal wind drag coefficient, f_{roll_i} is the rolling resistance coefficient, J_i is the wheel moment of inertia, r_i is the wheel radius, l_{f_i} is the distance from the front axle to the center of gravity (c.g.), l_{r_i} is the distance from the c.g. to the rear axle, and l_{h_i} is the vertical distance to the c.g. Note that, in model (1)–(6) a number of dynamical aspects, such as roll and yaw moments, lateral and vertical motions, brake, throttle, steering actuators and manifold dynamics, are neglected.

The wheel slip ratio of the i–th vehicle is defined as

$$\lambda_{f_i}=\frac{\omega_{f_i}r_{f_i}-v_{x_i}}{\max(\omega_{f_i}r_{f_i},v_{x_i})} \tag{7}$$

The slip ratio dynamics for the front and rear wheel can be obtained by differentiating λ_i with respect to time as

$$\begin{aligned}
\dot{\lambda}_{f_i} &= f_{f_i}(v_{x_i},\omega_{f_i},\lambda_{f_i},F_{xf_i})+h_{f_i}(v_{x_i},\omega_{f_i},\lambda_{f_i})T_{f_i} && (8)\\
\dot{\lambda}_{r_i} &= f_{r_i}(v_{x_i},\omega_{r_i},\lambda_{r_i},F_{xr_i})+h_{r_i}(v_{x_i},\omega_{r_i},\lambda_{r_i})T_{r_i} && (9)
\end{aligned}$$

where

$$\begin{aligned}
f_{f_i} &= -\frac{1}{\omega_{f_i}r_{f_i}}[-\frac{F_{loss_i}}{m_i}+\frac{2}{m_i}(F_{xf_i}+F_{xr_i})\\
&+\frac{v_{x_i}r_{f_i}}{J_{f_i}\omega_{f_i}}F_{xf_i}] && (10)\\
h_{f_i} &= \frac{v_{x_i}r_{f_i}}{J_{f_i}(\omega_{f_i}r_{f_i})^2} && (11)
\end{aligned}$$

Equations (10) and (11) are valid for the front wheel of the i–th vehicle in the acceleration case, but f_{f_i} and h_{f_i} can be similarly obtained in the deceleration case. The same holds for f_{r_i} and h_{r_i} in both the motion conditions.

As for the tire model, the well-known Bakker–Pacejka model [8] is considered in this paper (omitting the subscript f and r, since the treatment is identical for both the vehicle wheels), i.e.,

$$F_{x_i}=\mu_{p_i}f_{t_i}(\lambda_i,F_{z_i}) \tag{12}$$

where $\mu_{p_i}\in[0,1]$ is the tire–road adhesion coefficient, which depends on the road conditions. Typical value for μ_p are, for instance, 0.85, 0.6, and 0.3 which are associated with the case of dry asphalt, wet asphalt and snowy road, respectively [8]. Fig. 3 shows λ–F_x curves for different values of μ_p when F_z is fixed. In order to identify the λ–F_x curve corresponding to the current driving condition, it is necessary to determine the tire/road adhesion coefficient μ_{p_i} on the basis of the data acquired by the sensors. Following the approach proposed in [13], this parameter is estimated on–line using a recursive least–square scheme with forgetting factor.

III. The SOSM control design

A SOSM is a mode of a dynamic system confined to a subspace, the so–called sliding manifold, which can be

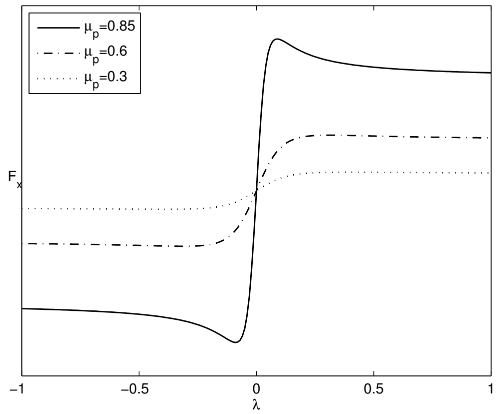

Fig. 3. λ–F_x curve for fixed F_z.

mathematically described in Filippovs' sense [7]. The SOSM is defined by

$$s(x) = \dot{s}(x) = 0 \tag{13}$$

where $s(x)$, the so–called sliding variable, is a smooth function of the state x of the considered dynamical system, and $s(x) = 0$ identifies the sliding manifold. SOSM control extends the basic sliding mode control idea, acting on the second order time derivative of the sliding variable, instead that on the first derivative, as it happens in first order sliding mode control design [4]. The main advantage of SOSM control, with respect to the first order case is that it generates a continuous control action, while keeping the same robustness with respect to matched uncertainties [2].

IV. The platooning problem

The outer loop of the proposed control scheme (see Fig 1) is designed to solve the platooning problem. The 0–th vehicle is the leader of the platoon, and its speed and acceleration are arbitrary, since it has no preceding vehicle to follow. The control objective of the i-th vehicle, with $i = 1, 2, \ldots, n$, is to maintain the safety distance from the preceding vehicle. In this paper, the safety distance is calculated in accordance to the Constant Time-Headway (CTH) policy, which is commonly suggested as a safe practice for human drivers and is frequently used in ACC designs [3]. The safety distance given by such policy is

$$S_{d_i}(v_{x_i}(t)) = S_{d_0} + h v_{x_i}(t) \tag{14}$$

where S_{d_0} is a lower bound of the safety distance, and h is the so–called headway time. Thus, considering the i–th vehicle, with $i = 1, 2, \ldots, n$, the spacing error is given by

$$e_i(t) = S_{d_0} + h v_{x_i}(t) - x_{i-1}(t) + x_i(t) \tag{15}$$

where $x_i(t)$ is the longitudinal position of the i–th vehicle and $x_{i-1}(t)$ is the longitudinal position of the $(i-1)$–th vehicle. The chosen sliding variable is just the spacing error, i.e.,

$$S_i(t) = e_i(t) = x_i(t) - x_{i-1}(t) + S_{d_0} + h v_{x_i}(t) \tag{16}$$

and its first and second time derivatives are

$$\left\{ \begin{array}{lll} \dot{S}_i(t) & = & \dot{e}_i(t) = v_{x_i}(t) - v_{x_{i-1}}(t) + h\dot{v}_{x_i}(t) \\ \ddot{S}_i(t) & = & \ddot{e}_i(t) = \dot{v}_{x_i}(t) - \dot{v}_{x_{i-1}}(t) + h\ddot{v}_{x_i}(t) \\ & = & \varepsilon_i(t) + w_i(t) \end{array} \right. \tag{17}$$

where $\varepsilon_i(t) = \dot{v}_{x_i}(t) - \dot{v}_{x_{i-1}}(t)$, and signal $w_i(t) = h\ddot{v}_{x_i}(t)$ can be regarded as an auxiliary control input. The term ε_i in (17) represents the difference between the longitudinal acceleration of two adjacent vehicles, which is bounded by mechanical and physical limits [8], i.e.,

$$|\varepsilon_i| \le \Gamma_i \qquad i = 1, \ldots, n \tag{18}$$

Then, to solve the platooning problem, the auxiliary control input is designed as

$$w_i(t) = -W_{M_i}\, sign\big[S_i(t) - \frac{1}{2} S_{i_{Max}}(t)\big] \tag{19}$$

with the constraint

$$W_{M_i} > 2\Gamma_i \tag{20}$$

where $S_{i_{Max}}(t)$ is a piece–wise constant function representing the value of the last singular point of $S_i(t)$ (i.e., the most recent value $S_i(t)$ such that $\dot{S}_i(t) = 0$). The control law can be analysed in analogy with that presented in [1]. In particular, it can be proved that the control law (19) causes the generation of a trajectory in the $S_i O \dot{S}_i$ plane with a sequence of states with coordinates $(S_{i_{Max_j}}; 0)$ featuring the following contraction property:

$$|S_{i_{Max_{j+1}}}| \le \alpha |S_{i_{Max_j}}| \;\; j = 1, 2, \ldots;\; \alpha \in [0; 1). \tag{21}$$

where $S_{i_{Max_j}}$ is the j–th extremal value of the signal $S_{i_{Max}}$. Moreover, the convergence of the system trajectory to the origin of the plane $S_i O \dot{S}_i$ takes place in finite time. From (16), this implies that the spacing error between the i–th and the $(i-1)$–th vehicle, and its first time derivative are steered to zero in finite time, i.e., $e_i = \dot{e}_i = 0$. Relying on (19) and (1), it is possible to determine the desired traction force for the i–th vehicle, i.e.,

$$F_{xf_{des_i}}(t) + F_{xr_{des_i}}(t) = \frac{1}{2}[m_i \dot{v}_{x_{des_i}}(t) + F_{loss_i}(v_{x_i}(t))] \tag{22}$$

where $\dot{v}_{x_{des_i}}(t)$ is calculated as

$$\dot{v}_{x_{des_i}}(t) = \frac{1}{h} \int_{t_0}^{t} w_i(\tau)\, d\tau \tag{23}$$

The next step consists in calculating of the desired slip ratios $\lambda_{f_{des_i}}$ and $\lambda_{r_{des_i}}$ from the desired traction force $F_{xf_{des_i}} + F_{xr_{des_i}}$. From (12), in the acceleration case, the following relationship should be maintained

$$F_{xf_i} \;\le\; \mu_{p_i} F_{zf_i} \tag{24}$$

$$F_{xr_i} \;\le\; \mu_{p_i} F_{zr_i} \tag{25}$$

By substituting (5) and (6) in (24) and (25), it yields

$$F_{xf_i} \;\le\; \mu_{p_i} \frac{l_{r_i} m_i g - 2 l_{h_i} F_{xr_i} + l_{h_i} F_{loss_i}}{2(l_{f_i} + l_{r_i} + \mu_{p_i} l_{h_i})} \tag{26}$$

$$F_{xr_i} \;\le\; \mu_{p_i} \frac{l_{r_i} m_i g + 2 l_{h_i} F_{xf_i} - l_{h_i} F_{loss_i}}{2(l_{f_i} + l_{r_i} - \mu_{p_i} l_{h_i})} \tag{27}$$

The optimal tire force distribution to achieve the best acceleration response is calculated as

$$\frac{F_{xf_i}}{F_{xr_i}} = \frac{l_{r_i} + l_{h_i}\frac{F_{loss_i}}{m_i g} + \mu_{p_i} l_{h_i}}{l_{f_i} - l_{h_i}\frac{F_{loss_i}}{m_i g} - \mu_{p_i} l_{h_i}} \tag{28}$$

which corresponds to the intersection point of the two boundary lines of (26) and (27). The optimal tire force distribution for the deceleration case can be similarly obtained. From (28) and (12), $\lambda_{f_{des_i}}$ and $\lambda_{r_{des_i}}$ are calculated as the slip ratios necessary to produce the desired traction force.

V. The slip controller

The slip controller has the objective of attaining the desired slip ratios $\lambda_{f_{des_i}}$, and $\lambda_{r_{des_i}}$ produced by the outer control loop as discussed in the previous section. In the sequel, for the sake of simplicity, a single vehicle is considered and the subscript i is omitted. The sliding variables are the slip tracking error at the front and rear wheel, respectively, i.e.,

$$\lambda_{je}(t) = \lambda_j(t) - \lambda_{j_{des}}(t) \qquad j \in \{f, r\} \tag{29}$$

since now the control objective is to steer these errors to zero. Then, the sliding manifolds are given by

$$s_j(t) = \lambda_{je}(t) = 0 \qquad j \in \{f, r\} \tag{30}$$

From (8) and (9), the first and second time derivatives of the sliding variables are

$$\left\{ \begin{array}{lcl} \dot{s}_j(t) & = & f_j(t) + h_j(t)T_j(t) - \dot{\lambda}_{j_{des}}(t) \\ \ddot{s}_j(t) & = & \dot{f}_j(t) + \dot{h}_j(t)T_j(t) + h_j(t)\dot{T}_j(t) - \ddot{\lambda}_{j_{des}}(t) \\ & = & \varphi_j(t) + \gamma_j(t)\dot{T}_j(t) \qquad j \in \{f, r\} \end{array} \right. \tag{31}$$

where $\varphi_j(t) = \dot{f}_j(t) + \dot{h}_j(t)T_j(t) - \ddot{\lambda}_{j_{des}}(t)$, and $\gamma_j(t) = h_j(t)$. On the basis of straightforward physical considerations, it turns out that the quantities $\varphi_f(t)$, and $\varphi_r(t)$ are bounded. Moreover, it can be assumed that suitable bounds of $\varphi_j(t)$, $j \in \{f, r\}$, i.e.,

$$\Phi_j \quad \geq \quad |\varphi_j(t)| \qquad j \in \{f, r\} \tag{32}$$

are known. These bounds can be determined on the basis of (10), (11), the analogous relationships written for the rear wheel, and the limit characteristic curves of the input torques which the engine can transfer to the wheels. Similar considerations can be made for $\gamma_f(t)$, and $\gamma_r(t)$, which can be regarded as unknown bounded functions with the following known bounds

$$0 < \Gamma_{j1} \leq \gamma_j(t) \leq \Gamma_{j2} \qquad j \in \{f, r\} \tag{33}$$

Taking into account system (31) for which (32), and (33) hold, in order to generate second order sliding modes on the manifolds (30), the control variable $T_j(t)$, $j \in \{f, r\}$, are designed as

$$\dot{T}_j(t) \;=\; -\alpha_j(t) V_{jM}\, sign\left[s_j(t) - \frac{1}{2} s_{jM}(t)\right] \quad j \in \{f, r\} \tag{34}$$

$$\alpha_j(t) \;=\; \left\{ \begin{array}{lll} \alpha_j^* & if & [s_j(t) - \frac{1}{2}s_{jM}(t)][s_{jM}(t) - s_j(t)] > 0 \\ 1 & if & [s_j(t) - \frac{1}{2}s_{jM}(t)][s_{jM}(t) - s_j(t)] \leq 0 \end{array} \right.$$

$$j \;\in\; \{f, r\}$$

with the constraints

$$\begin{array}{ll} \alpha_j^* \in (0,1] \cap (0, \frac{3\Gamma_{j1}}{\Gamma_{j2}}) & j \in \{f, r\} \\ V_{jM} > \max\{\frac{\Phi_j}{\alpha_j^* \Gamma_{j1}}, \frac{4\Phi_j}{3\Gamma_{j1} - \alpha_j^* \Gamma_{j2}}\} & j \in \{f, r\} \end{array} \tag{35}$$

where $s_{jM}(t)$ is a piece–wise constant function representing the value of the last singular point of $s_j(t)$ (i.e., the most recent value $s_j(t)$ such that $\dot{s}_j(t) = 0$). In accordance with [1], it can be proved that the trajectories on the $s_j O \dot{s}_j$ ($s_r O \dot{s}_r$) plane are confined within limit parabolic arcs which include the origin. Moreover, the origin of the plane, i.e. $s_f = \dot{s}_f = 0$ ($s_r = \dot{s}_r = 0$), is reached in a finite time, so that the control objective of tracking the desired slip is attained. Note that the stability of the overall control system in Fig 1 could be also studied by considering together the two coupled systems (17) and (31). Yet, the coupling terms is dominated by the discontinuous control action $\dot{T}_j(t)$. This is the reason why he stability of the control scheme in Fig. 1 has been discussed by considering the dynamics of the two errors separately.

VI. Comments on the controllers

The proposed controllers generate continuous control signals, thus avoiding the necessity of approximating the discontinuous signals so as to reduce the actuators stress and the induced vibrations, as required in conventional discontinuous sliding mode controllers. As one can note, the control law only requires the knowledge of the extremal value of the sliding variables, i.e., $S_{i_{Max}}$, $s_{fi_{Max}}$, and $s_{ri_{Max}}$, which implies the capability to identify the time instants when the first time derivatives of the sliding variables are crossing zero. For instance, a possibility to evaluate the extremal value of the sliding variable S_i is to determine the quantity

$$\Delta(t) = [S_i(t - \delta) - S_i(t)]S_i(t) \tag{36}$$

where δ is an arbitrarily small time delay [1]. This means that, even if $\dot{S}_i$ is not available for measurements, its sign can be indirectly determined by observing the sign of both $S_i(t)$ and $\Delta(t)$. The extremal values of $s_{fi_{Max}}$, and $s_{ri_{Max}}$ can be detected similarly. If the extremal values of the sliding variables are evaluated with (36), the control laws proposed in this paper, with minor modifications, cause the finite–time convergence of the system to a δ-vicinity of the origin of the error plane, in analogy with [1]. Note that, relying on the control variables T_{fi} and T_{ri}, the total available braking torque T_{brake_i}, and the engine torque exerted on the driving shaft T_{shaft_i} can be calculated. In a more complete view of the vehicle control system, T_{brake_i}, and T_{shaft_i} need to be regarded as reference signals for the throttle angle controller and for the brake controller, respectively [14].

VII. Simulation results

The platoon considered in this simulation is composed of two front–wheel–driven cars (FWD). Since there is only one follower vehicle, in the sequel the subscript i will be omitted. In the case of a FWD vehicle, the possible distribution of T_{fi} and T_{ri} is [14]

$$T_f \;=\; 0.5T_{shaft} - 0.3T_{brake} \tag{37}$$

$$T_r \;=\; -0.2T_{brake} \tag{38}$$

TABLE I

SIMULATION PARAMETERS

g	9.81	m/s^2
m	1202	kg
J_f	1.07	kgm^2
J_r	1.07	kgm^2
c_x	0.4	
f_{roll}	0.013	
r_f	0.32	m
r_r	0.32	m
l_f	1.15	m
l_r	1.45	m
l_h	0.65	m
$v_x(0)$	30	m/s
$\lambda_f(0)$	0.01	
$\lambda_r(0)$	0.01	

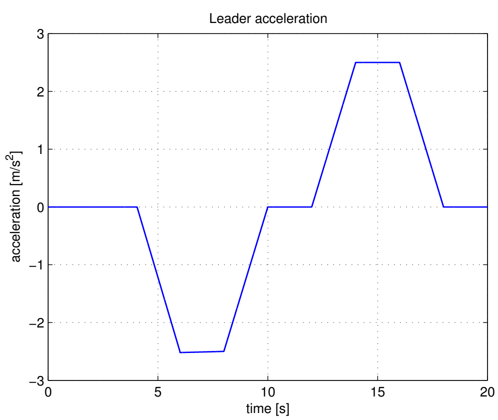

Fig. 4. The acceleration profile of the leader vehicle.

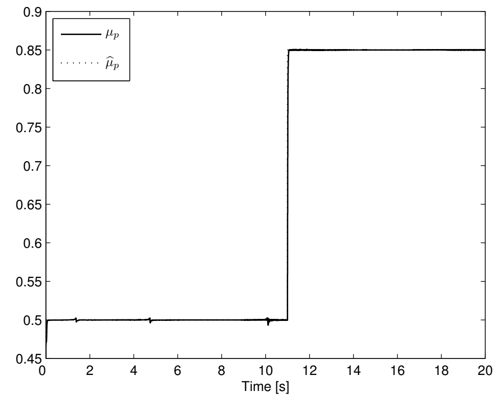

Fig. 5. The actual μ_p value versus its estimated value $\hat{\mu}_p$.

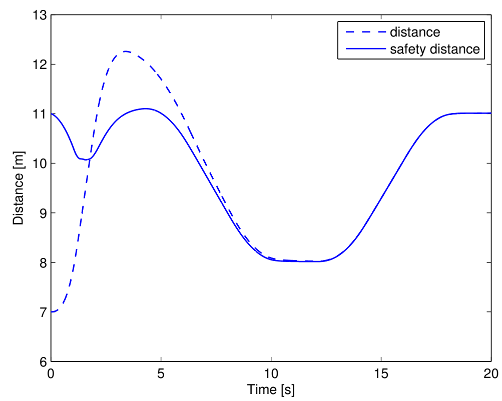

Fig. 6. Time evolution of the distances between the two vehicles.

For the sake of simplicity, the vehicles are supposed to be identical and the parameters of the model used in simulation are indicated in Tab. I. Both the leader and the follower vehicle have an initial velocity of $30m/s$. The acceleration of the leader vehicle is shown in Fig 4. The initial distance between the two vehicles is $7m$ and the safety distance is calculated in accordance to (14) with $S_{d_0} = 2m$ and $h = 0.3s$. In the simulated scenario, the road condition is assumed to change at $t = 11s$ from wet asphalt ($\mu_p(wet) = 0.5$) to dry asphalt ($\mu_p(dry) = 0.85$). The parameter μ_p is correctly estimated by the recursive least–square algorithm with forgetting factor, as shown in Fig. 5. The evolution in time of the distance between the leader and the follower vehicle is shown in Fig 6. One can note that the safety distance between vehicles is reached in finite time, as expected. Figs. 7 and 8 show the evolution in time of the sliding variable s_f and s_r, respectively. As expected, the sliding manifolds defined by $s_f = 0$, and $s_r = 0$ are reached in finite time. When the road condition changes, the desired slip ratio change consequently, and is tracked correctly again after a finite time. The evolution of the variables T_{shaft} and T_{brake} are shown in Fig. 9 and (10), respectively.

VIII. CONCLUSIONS

In this paper a robust longitudinal control scheme for platoons of vehicles has been proposed. The control objective is to make the controlled vehicle travel maintaining the desired safety distance with respect to the preceding vehicle. Since the traction force depends on the wheel slip ratio, the desired traction force can be achieved by controlling the slip ratio. An adaptive algorithm is adopted to take into account the unknown and time–varying tire/road adhesion coefficient. The controller of each controlled vehicle of the platoon, is designed so as to generate second order sliding modes on suitable manifolds. The choice of the SOSM control methodology is motivated by its robustness against disturbances, model inaccuracies, and parameter variations which are rather typical in the automotive context. The proposed SOSM controllers generate continuous control actions, thus limiting actuator stress and the vibrations they can induce and propagate throughout the vehicle subsystems. Simulation results have demonstrated the possible effectiveness of the proposal. Yet, future works need to be devoted to verify the performances of the designed vehicle controller applied to a more accurate model of the vehicle than that considered in this paper. In particular, it seems important to analyze the coupling of the proposed longitudinal control scheme with

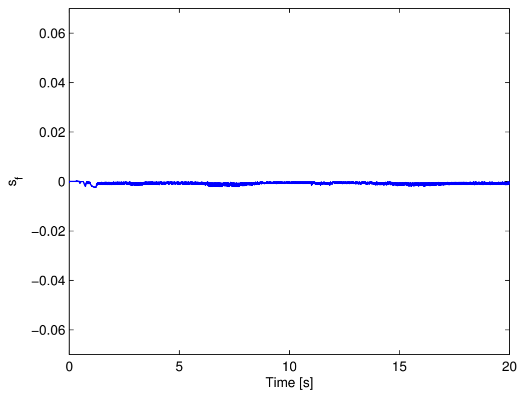

Fig. 7. Time evolution of s_f.

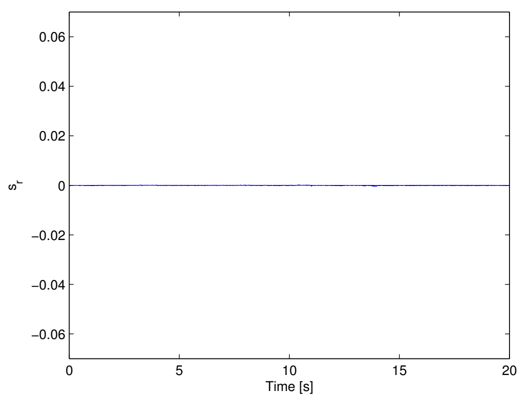

Fig. 8. Time evolution of s_r.

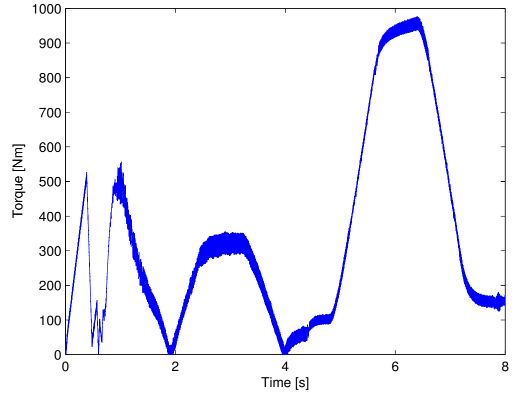

Fig. 9. The time evolution of the produced engine torque T_{shaft}.

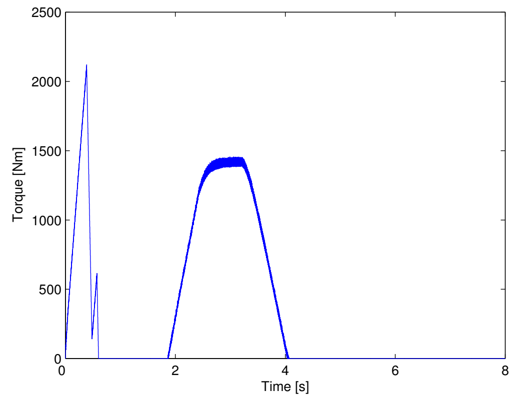

Fig. 10. The time evolution of the applied braking torque T_{brake}.

throttle angle and brake controllers, taking into account the actuators dynamics which is neglected in the present paper.

REFERENCES

[1] G. Bartolini, A. Ferrara and E. Usai,"Output tracking control of uncertain nonlinear second-order systems," *Automatica*, vol. 33, no. 12, pp. 2203–2212, 1997.

[2] G. Bartolini, A. Ferrara, F. Levant and E. Usai, "On second order sliding mode controller," in *Variable Structure Systems, Sliding Mode and Nonlinear Control*, K–K. David Young and Ü. Özgüner Eds. Lecture Notes in Control and Information Sciences, Springer–Verlag, vol. 247, pp. 329–350, 1999.

[3] Chien C.C., Ioannou P. and Lai M.C., "Entrainment and vehicle following controllers design for autonomous intelligent vehicles," *Proc. American Control Conference*, pp. 6–10, Baltimore, Maryland, USA, 1994.

[4] C. Edwards and K. S. Spurgeon, *Sliding Mode Control: Theory and Applications*. Taylor & Francis, London, UK, 1998.

[5] A. Ferrara and P. Pisu, "Minimum sensor second-order sliding mode longitudinal control of passenger vehicles," *IEEE Transactions On Intelligent Transportation Systems*, vol. 5, no. 1, pp.20–32, 2004.

[6] Ferrara A. and C. Vecchio, "Controlling a platoon of vehicles via second order sliding mode approach," *CTS 2006 11th IFAC Symposium on Control in Transportation Systems*, Delft, The Netherlands, 2006.

[7] A. F. Filippov, *Differential Equations with Discontinuous Right–Hand Side*. Kluwer, Dordrecht, the Netherlands, 1988.

[8] G. Genta, *Motor Vehicle Dynamics. Modeling and Simulation*. World Scientific, 1997.

[9] I. Haskara, C. Hatipoglu and Ü. Özgüner, "Sliding mode compensation, estimation and optimization methods in automotive control," in *Variable Structure Systems, Sliding Mode and Nonlinear Control*, K–K. David Young and Ü. Özgüner Eds. Lecture Notes in Control and Information Sciences, Springer–Verlag, vol. 247, pp.155–174, 2002.

[10] I. Haskara, Ü. Özgüner and J. Winkelman, "Wheel slip control for antispin acceleration via dynamic spark advance," *Control Engineering Practice*, vol. 8, no. 10, pp.1135–1148, 2000.

[11] M. Kabganian and R. Kazemi, "A new strategy for traction control in turning via engine modeling," *IEEE Transactions On Vehicular Technology*, vol. 50, no. 6, pp.1540–1548, 2001.

[12] S. M. Kang, M. Yoo and M. Sunwoo, "Traction control using a throttle valve based on sliding mode control and load torque estimation," *Journal of Automobile Engineering*, pp. 645–653, 2005.

[13] H. Lee and M. Tomizuka, "Adaptive vehicle traction force control for intelligent vehicle highway systems (IVHSs)," *IEEE Transactions on Industrial Electronics*, vol. 50, no. 1, pp.37–47, 2003.

[14] H. Lee, D. Love and M. Tomizuka, "Longitudinal maneuvering control for automated highway systems based on a magnetic reference/sensing system," in *Proc. of 1995 American Control Conference*, Seattle, WA, pp.150–154, 1995.

[15] S. E. Shladover, C. A. Desoer, J. K. Hedrick, M. Tomizuka, J. Walrand, W.-B. Zhang, D. H. McMahon, H. Peng, S. Sheikholeslam, and N. McKeown, "Automatic vehicle control developments in the PATH program," *IEEE Transactions on Vehicular Technology*, vol. 40, no. 1, pp.114–130, 1991.

[16] M. Tomizuka, J. K. Hedrick and H. Pham, "Integrated manoeuvring control for automated highway systems based on magnetic reference/sensing system," Univ. California, Berkeley, CA, *PATH Rep. UCB-ITS-PRR-95-12*, 1995.

[17] V.I. Utkin, *Sliding Modes in Control and Optimization*, Springer–Verlag, New York, 1992.

[18] L. Xy, H. S. Tan, S. E. Shladover and J. K. Hedrick, "Nonlinear longitudinal controller implementation and comparison for automated cars," *Journal of Dynamic Systems Measurement and Control*, vol. 123, no. 2, pp. 161–167, 2001.